

# Macroautophagy supports Sonic Hedgehog signaling by promoting Patched1 degradation

Xin Yang<sup>a,1</sup>, Nan Jin<sup>b,1</sup>, Yu Wang<sup>a,1</sup>, Yixing Yao<sup>a,c</sup>, Yue Wang<sup>a</sup>, Tianyuan Li<sup>a</sup>, Chen Liu<sup>a</sup>, Tingting Yu<sup>a</sup>, Hao Yin<sup>b</sup>, Ziyu Zhang<sup>a,d,\*</sup>, Steven Y. Cheng<sup>a,e,\*</sup>, Shen Yue<sup>a,d,\*</sup>

<sup>a</sup> Department of Medical Genetics, Jiangsu Key Laboratory of Xenotransplantation, Nanjing Medical University, Nanjing 211166, China

<sup>b</sup> The First School of Clinical Medicine, Nanjing Medical University, Nanjing 211166, China

<sup>c</sup> Department of Pathology, Suzhou Ninth People's Hospital, Suzhou 215200, PR China

<sup>d</sup> Key Laboratory of Women's Reproductive Health of Jiangxi, Jiangxi Maternal & Child Health Hospital, Nanchang, Jiangxi 330006, PR China

<sup>e</sup> Jiangsu Key Lab of Cancer Biomarkers, Prevention and Treatment, Collaborative Innovation Center for Cancer Personalized Medicine, Nanjing Medical University, Nanjing 211166, China

## ARTICLE INFO

### Keywords:

Autophagy  
Primary cilia  
Patched1  
Degradation  
Shh signaling

## ABSTRACT

Autophagy is a highly conservative self-digestion process to maintain intracellular homeostasis and to ensure the survival of cells under stress. Activation of Sonic Hedgehog (Shh) signaling depends on the normal endocytic degradation of pathway receptor Patched1 (Ptch1). It is unclear whether autophagy participates in the receptor endocytosis and modulates Shh signaling transduction. Here we found that blocking macroautophagy attenuates Shh signaling due to the failed transport of Smoothened (Smo) into primary cilia. At the upstream of Smo, Ptch1 was poly-ubiquitinated through K63-conjugated ubiquitin chains. Macroautophagy participates Shh-induced degradation of poly-ubiquitinated Ptch1, contributing to the activation of Shh signaling.

## 1. Introduction

Autophagy is an evolutionarily conserved process occurs in almost all eukaryotic cells, of great significance to maintain intracellular homeostasis by degrading and recycling long-lived proteins and dysfunctional organelles [1,2]. There are three general types of autophagy, including macroautophagy, microautophagy and chaperone-mediated autophagy, depending on the mechanism of cargo delivery to lysosomes for degradation [3]. Macroautophagy initiates with the nucleation of the phagophores, the membrane-like structures in the cytoplasm [4]. The phagophores continue to expand and thus complete the formation of autophagosomes, the double-membrane vesicles, to sequester cargo and transport it to lysosomes [5]. LC3II, a lipidated form of LC3, is attached to the phagophore membrane and contributes to the expansion of phagophores. It is subsequently removed from the autophagosome outer membrane, which is followed by fusion of the autophagosome with a lysosome to form autolysosome [6,7]. P62 works as a major cargo receptor to target the ubiquitinated cargos to the LC3II-decorated autophagosome for degradation [8,9]. Ultimately the encompassed cargos are degraded in autolysosomes to meet the metabolic needs and

renew organelles [10,11].

Sonic Hedgehog (Shh) plays an instrumental role in many fundamental processes of embryonic development by specifying the patterns of cell growth and differentiation [12,13]. Loss of, or interference with, Shh signaling function results in a myriad of developmental defects such as holoprosencephaly, cyclopia, and limb abnormalities. Aberrant activation of Shh signaling contributes to a variety of malignant cancers [14]. Shh signaling is initiated by the binding of Shh ligand to the 12-pass transmembrane receptor Patched-1 (Ptch1) [15,16]. The binding induces degradation of Ptch1, attenuates the inhibition of Ptch1 on Smoothened (Smo) [17,18], and promotes Smo to accumulate within primary cilia leading to the activation of the Gli family of transcription factors [19]. Suppressor of fused (Sufu) is a binding partner of Gli proteins and negatively regulates the pathway [20]. Although precise temporal and spatial control of Shh signaling is essential, the detailed mechanism remains elusive.

Controllable protein degradation is essential for the regulation of Shh signaling transduction. Autophagy and ubiquitin-proteasome system (UPS) are two main protein degradation systems despite their distinct degradation mechanisms. Ubiquitination is a reversible covalent

\* Corresponding authors at: Department of Medical Genetics, Jiangsu Key Laboratory of Xenotransplantation, Nanjing Medical University, Nanjing 211166, China. E-mail addresses: [airity@163.com](mailto:airity@163.com) (Z. Zhang), [syeheng@njmu.edu.cn](mailto:syeheng@njmu.edu.cn) (S.Y. Cheng), [yueshen@njmu.edu.cn](mailto:yueshen@njmu.edu.cn) (S. Yue).

<sup>1</sup> equally contributed in this study.

modification via three enzymatic steps [21]. Ubiquitinated substrates are recognized by specific adaptors and then delivered to the proteasome or autophagosomes for degradation. Moreover, some ubiquitin linkages regulate the interactions and biological functions of substrates through non-proteolytic processes. In poly-ubiquitinated proteins, the ubiquitin chains can be linked through any of its seven Lysine residues (K6, K11, K27, K29, K33, K48, and K63) or N-terminal Methionine (M1). Among them, K48- and K63- linked poly-ubiquitination are the most predominant poly-ubiquitination types [22]. Our previous study has revealed that Shh promotes the degradation of the pathway upstream receptor — Ptc1 and the downstream essential regulator — Sufu through UPS [23]. The transcription factors Gli1 and Gli2 are also reported to be ubiquitinated and degraded, the balance between their ubiquitination and de-ubiquitination plays a critical role for proper transcription of Shh target genes [24,25].

UPS and autophagy were historically believed to function in parallel in the cell but accumulating evidence shows a dynamic cross-talk between UPS and autophagy recently, such as sharing molecular determinants ubiquitin and substrates p62 [26]. Given the important roles of autophagy, we set out to investigate the effect of autophagy in the regulation of Shh signaling by ubiquitination. Here, we provide the evidence that macroautophagy participates Shh signaling by promoting Ptc1 degradation.

## 2. Materials and methods

### 2.1. Cells, plasmids and siRNAs

Immortalized wild-type (WT) and *Gli3*<sup>-/-</sup> mouse embryo fibroblasts (MEFs) were generous gifts from the Wade Bushman laboratory. *Sufu*<sup>-/-</sup>, *Ptc1*<sup>-/-</sup> MEFs were described previously [27]. HEK293 cells were purchased from ATCC. Full-length mouse Ptc1 cDNA was obtained from ATCC, and the GFP-tagged Ptc1 and 6 × Flag-tagged Ptc1 were generated by PCR and cloned into the pRK5 vector. All PCR-amplified fragments were sequence verified. Plasmids for GFP-tagged Ptc1 and HA-tagged Ubiquitin (Ub), UbK63, UbK48, UbK63R and UbK48R were described previously [28–32]. siRNA specific for the mouse Atg5 was purchased from Thermo Fisher Scientific.

### 2.2. Immunofluorescence staining

Approximately  $0.6 \times 10^5$  cells per well were seeded in Lab-Tek chambered slides and cultured for 24 h. The cells were transfected, allowed to recover for 24 h, and then treated with ShhN-CM or other compounds, as indicated. For visualizing ciliary proteins, the transfected cells were starved in DMEM (Dulbecco's modified Eagle's medium) containing 0.5% fetal bovine serum for 24 h before other treatments. The cells were fixed with 4% paraformaldehyde for 15 min at 4 °C, and standard procedures for immunostaining were followed. The primary antibodies were rabbit anti-IFT88 (Proteintech; 1:400), mouse anti-Smo (Santa Cruz Biotechnology; 1:50), mouse anti-acetylated  $\alpha$ -tubulin (Sigma; 1:1000), mouse anti-Flag (Sigma; 1:200), rabbit anti-LC3 (Proteintech; 1:200), rabbit anti-P62 (Proteintech; 1:100), and rabbit anti-NBR1 (Proteintech; 1:200). The secondary antibodies were Alexa Fluor-conjugated antibodies from Thermo Fisher Scientific (1:200).

### 2.3. Confocal microscopy

Confocal images were acquired on a Carl Zeiss LSM710 confocal microscope with a 63× 1.4 NA oil immersion objective, and were analyzed using Zeiss ZEN2011 program. Primary cilia stained with anti-acetylated  $\alpha$ -tubulin were traced from the base to the tip using the Open Bezier tool in Graphics toolbar. Cilia lengths were measured using simple line measurement tools of Zen software.

### 2.4. Immunoprecipitation and immunoblotting

Transfected cells were lysed in modified RIPA buffer (50 mM Tris-HCl, pH 7.4, 150 mM NaCl, 1% vol/vol NP-40, 1% n-Dodecyl  $\beta$ -D-maltoside, 0.25% wt/vol sodium deoxycholate, 1 mM DTT, and 1 × Roche complete Protease Inhibitor Cocktail) for 1 h at 4 °C. The lysate was clarified by centrifugation for 20 min at 14,000 ×g. The protein concentration was determined using a bicinchoninic acid assay and equal amounts of total protein from each of the samples was supplemented with 5 × SDS loading buffer, incubated at room temperature for 1 h, subjected to SDS-PAGE, followed by western blot analysis. To measure the interactions between exogenous Ptc1-GFP and HA-tagged Ub or its mutants, transfected Ptc1-GFP was immunopurified with anti-GFP antibodies coated Dynabeads™ Protein G (Thermo) and subjected to SDS-PAGE, followed by western blotting with mouse anti-HA (1:1000; Thermo). The following antibodies were used: rabbit anti-GFP for Ptc1-GFP (Abcam; 1:200), mouse anti- $\beta$ -actin (Santa Cruz Biotechnology; 1:1000), rabbit anti-Gli1 (Cell Signaling Technology; 1:1000), rabbit anti-LC3B (Cell Signaling Technology; 1:1000), rabbit anti-Atg5 (Proteintech; 1:500), rabbit anti-p62 (Cell Signaling Technology; 1:1000), mouse anti-HA (Sigma; 1:1000), mouse anti-Flag (Sigma; 1:1000) and rabbit anti-NBR1 (Proteintech; 1:500).

### 2.5. CRISPR-Cas9 genome editing

Genome editing was achieved using the CRISPR-Cas9 technique in MEFs. Briefly, a single-guide RNA (sgRNA) targeted the second and third exon of mouse Atg5 was designed and cloned into pX330 vector (from Addgene). The sgRNA sequences are: 5'- GUGCUUCGAGAUGUGUGGUU-3' and 5'- GAGAUUAUGGUUGAAUAUGA-3'. Cells were co-transfected with CRISPR/Cas9 plasmids and empty plasmids containing neomycin resistance genes. 48 h after transfection, transfected cells were selected using G418 (500  $\mu$ g/ml) for 5 days, followed by another 4 days without selection for expansion. Then the survived MEFs were seeded at 30 cells per well in 96-well plates and screened by PCR genotyping.

### 2.6. Reverse transcription (RT) and real-time PCR

Total RNAs were isolated from cultured cells with RNAiso Plus reagent (TaKaRa) and reverse transcribed using HiScript II Q RT SuperMix (Vazyme). Quantitative real-time PCR (qPCR) was carried out using AceQ qPCR SYBR Green Master Mix (Vazyme). Each measurement was repeated three times, and each sample was analyzed in triplicate with hypoxanthine phosphoribosyl transferase (HPRT) as an internal control. The qPCR primers are listed:

Mouse Gli1: Forward: 5'-TCCAGCTTGGATGAAGGACCTTGT -3'  
Reverse: 5'-AGCATATCTGGCAGGAGCATGTA-3'  
Mouse HPRT: Forward: 5'-TATGGACAGGACTGAAAGAC-3'  
Reverse: 5'-TAATCCAGCAGGTCAGCAAA-3'

### 2.7. Statistical analysis

Statistical analyses were performed with GraphPad Prism 7.0. Each measurement was repeated at least three times. Comparisons between indicated groups were performed using independent-samples *t*-test. *P* values <0.05 were considered statistically significant. \**P* < 0.05, \*\**P* < 0.01, and \*\*\**P* < 0.001. n.s. not significant.

## 3. Results

### 3.1. Impaired macroautophagy attenuates Shh signaling

To investigate whether macroautophagy has any effect on Shh signal transduction, we first used Bafilomycin A1 (BafA1) to inhibit fusion between autophagosomes and lysosomes in MEFs. Under BafA1 treatment,

LC3II was significantly accumulated (Fig. 1A, lane 4–6), meanwhile the autophagy substrate P62 was increased as well (Fig. 1A, lane 4–6). With the reduction of autophagy, the response to the stimulation of Shh ligand or Smo agonist SAG sharply declined in BafA1 treated MEFs. Western blotting indicated that Shh and SAG-induced production of Gli1 was apparently inhibited in BafA1 treated MEFs compared with untreated ones (Fig. 1A). BafA1 performed a stronger inhibitory effect on Shh-induced Gli1 expression. It is known that proteasome-dependent

degradation is essential for Shh signaling. Western blotting also showed that Shh and SAG failed to induce Gli1 production in MG132 treated MEFs (Fig. 1A). Furthermore, knockdown of Autophagy related 5 (Atg5), a core player in the extension of the phagophore membrane in autophagic vesicles, also curtailed Gli1 expression induced by Shh or SAG (Fig. 1B). Serum deprivation could induce macroautophagy and ciliogenesis as well. Our WB results showed the Shh and SAG stimulation induced much more Gli1 expression in serum starved MEFs than in

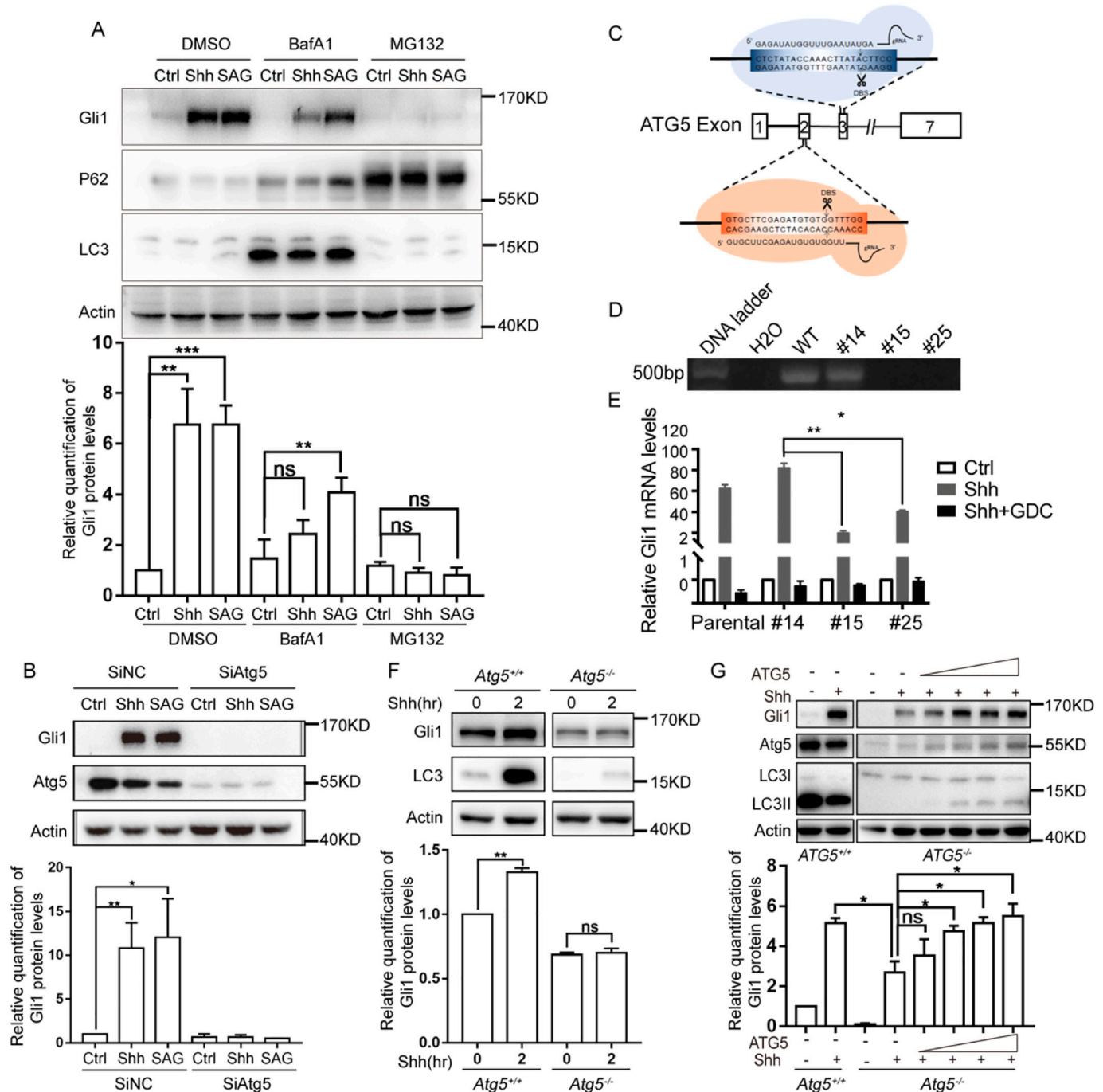


**Fig. 1.** Blocking autophagy pathway suppresses Shh signaling. (A) Western blot analysis of Gli1, P62, LC3II protein level in MEFs under BafA1 or MG132 treatment. The level of actin was used as a loading control. Quantification of Gli1 protein level normalized on actin and represented in bar graph. (B) Western blot and relative quantification of Gli1 protein level in MEFs transfected with *Atg5* siRNA. (C) CRISPR-Cas9 genome editing pattern of *Atg5*. (D) Identification of *Atg5* genotype. (E) QPCR analyses of Gli1 mRNA level in *Atg5*<sup>+/+</sup> and *Atg5*<sup>-/-</sup> MEFs after treated with Shh or Smo specific antagonist GDC-0449 (GDC) for 24 h. (F) Western blot analysis and relative quantification of Gli1 protein level in *Atg5*<sup>+/+</sup> and *Atg5*<sup>-/-</sup> MEFs after 2 h Shh stimulation. (G) Western blot analysis of Gli1 and LC3II protein levels after returning *Atg5* plasmids into *Atg5*<sup>-/-</sup> cells, treated with Shh for 24 h. Quantification of Gli1 expression represented in bar graph. Data in bar graphs are expressed as mean  $\pm$  SEM. \*  $P < 0.05$ , \*\*  $P < 0.01$ .

regular cultured cells (shown in Supplementary Fig. 1A). Therefore, the above and subsequent experiments were done in the absence of serum.

In addition, clustered regularly interspersed short palindromic repeat (CRISPR) - CRISPR-associated protein 9 (Cas9) genome editing was used to knockout *Atg5* in MEFs. CRISPR-Cas9 sgRNAs targeting the second and third exon of murine *Atg5* gene were generated (Fig. 1C), and then introduced into MEF cells. Through PCR-based genotyping, we identified clone #15 and #25 as *Atg5*<sup>-/-</sup> MEFs (Fig. 1D). Western blotting also confirmed the loss of *Atg5* protein expression in edited MEFs (Fig. 1G), proving that we have succeeded in building knockout cells. In addition to being a transcription factor of Shh pathway, Gli1 acts also as a Gli target gene. Then we quantified the transcription responses to Shh ligand stimulation in *Atg5*<sup>-/-</sup> MEFs by Gli1 RT-qPCR, and found that Shh-induction of target gene Gli1 was apparently inhibited in *Atg5*<sup>-/-</sup> MEFs compared with parental MEFs or *Atg5*<sup>+/+</sup> CRISPR clone #14 (Fig. 1E), suggesting that Shh fails to activate Gli transcription factors without *Atg5*. Consistent with this, Western blotting showed failed induction of Gli1 and LC3II in *Atg5*<sup>-/-</sup> cells after 2 h stimulation of

Shh in low serum condition (Fig. 1F). More importantly, to exclude the possible off-target effect of CRISPR-Cas9 editing, we re-introduced *Atg5* cDNA into *Atg5*<sup>-/-</sup> MEFs with a gradient dose (0.125–1  $\mu$ g) to rescue the protein activity. The re-introduction rescued Shh-induced Gli1 expression (Fig. 1G, lane 5–8), demonstrating the involvement of *Atg5* in Shh signaling. Collectively, these results showed that blocking macroautophagy pathway suppresses Shh signaling.

### 3.2. The biogenesis of primary cilia is not affected in autophagy-deficient cells

Although we have known macroautophagy plays an important role in Shh signaling, the mechanism remains to be clarified. It has been identified that primary cilia, the microtubule-based organelles that extend from the surface of the most vertebrate cells, have an essential role in Shh signaling [33]. Macroautophagy was reported to promote primary ciliogenesis by removing a ciliopathy protein, OFD1 (oral-facial-digital syndrome 1), from centriolar satellites [34]. However,

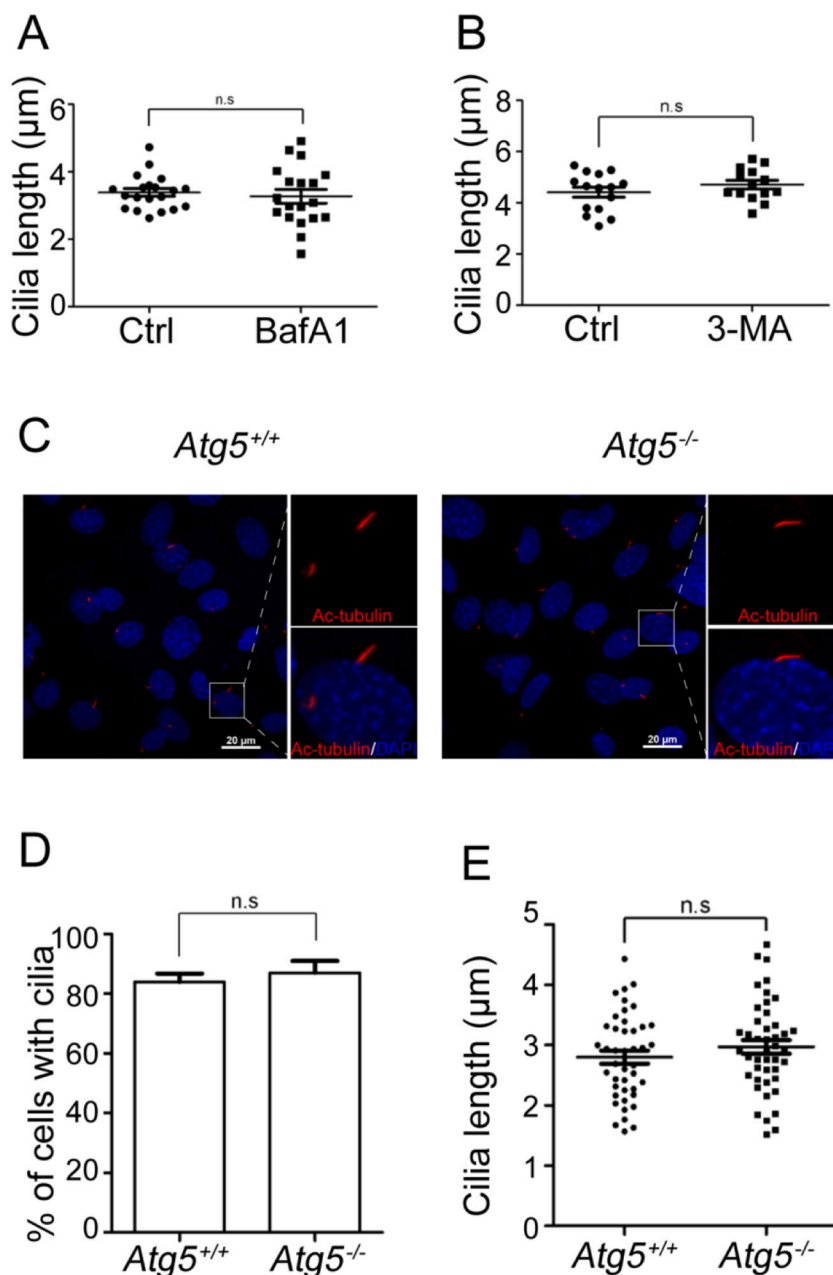


**Fig. 2.** Blocking autophagy does not affect cilia growth. Quantification of cilia length of ciliated MEFs after treatment with BafA1 (A) and 3MA (B) respectively. The cells were pre-treated with 0.5% FBS for 24 h to induce cilia growth. Primary cilia were stained by anti-acetylated tubulin. (C) Representative confocal images of anti-acetylated tubulin (red) showing primary cilium in *Atg5*<sup>+/+</sup> and *Atg5*<sup>-/-</sup> MEFs. Nucleus are stained with DAPI (blue). Quantitation of percentage (D) and ciliary length (E) of ciliated cells from (C). Data in bar graphs are expressed as mean  $\pm$  SEM. n.s. not significant.



basal autophagy was reported to inhibit ciliogenesis by limiting trafficking to the cilium of components required for ciliary growth [35]. Thus, we hypothesize that the attenuated Shh signaling in our *Atg5*<sup>-/-</sup> MEFs may be due to defects of ciliary growth. To attest the above possibility, we measured the physical properties of primary cilium in MEFs either treated with macroautophagy blockers or knocked out of *Atg5* gene. Unexpectedly, inhibition of macroautophagy with BafA1 did not interrupt the cilia growth in MEFs upon serum removal. The length of the cilia is comparable to those formed in untreated MEFs (Fig. 2A). The class III phosphoinositide 3-kinase inhibitor 3-methyladenin (3-MA), inhibit the initial phase of the autophagic process, did not affect the cilia growth in MEFs either (Fig. 2B). Also, around 80% of *Atg5*<sup>-/-</sup> MEFs formed a cilium after 30 h of serum starvation (Fig. 2C). *Atg5* depletion did not affect the number of ciliated MEF cells and the cilia length either (Fig. 2D, E). These results excluded the possibility that defects in ciliary biogenesis disturb Shh signal transduction.

### 3.3. Smo failed to localize into primary cilia in macroautophagy-deficient cells

Shh stimulation triggers the translocation of Smo into the primary cilium, which activates the downstream Gli transcription factors. To understand whether Shh-induced accumulation of Smo in primary cilia is manipulated by macroautophagy, we examined ciliary staining of Smo

in MEFs under Shh stimulation. It was found that BafA1 and 3-MA (Fig. 3A, B) attenuated the localization of Smo in primary cilia in the presence of ShhN. Shh also failed to induce Smo trafficking in *Atg5*<sup>-/-</sup> MEFs. The intensity of Smo staining in cilia was dramatically reduced in *Atg5*<sup>-/-</sup> MEFs compared to *Atg5*<sup>+/+</sup> MEFs (Fig. 3C, D). These data suggested that the blockade of macroautophagy obstructs the ciliary trafficking of Smo in primary cilia although the ciliogenesis is unaffected. It is also suggested that macroautophagy modifies Shh signaling at the upstream of Smo.

### 3.4. Macroautophagy participates Shh-induced *Ptch1* degradation

In order to further explore which mediator of Shh pathway might be regulated by macroautophagy, we knock down *Atg5* with siRNA in a panel of mutant MEF cells lacking different Shh signaling repressors. Shh pathway is continuously activated in *Ptch1*<sup>-/-</sup>, *Sufu*<sup>-/-</sup> and *Gli3*<sup>-/-</sup> MEFs in the absence of ShhN. Knockdown of *Atg5* did not reduce the expression of Gli1 in *Ptch1*<sup>-/-</sup> MEFs (Fig. 4A). Meanwhile, siRNA depletion of *Atg5* also failed to reduce Gli1 levels in *Sufu*<sup>-/-</sup> or *Gli3*<sup>-/-</sup> MEFs. Combining with the previous findings that blocking macroautophagy inhibits the Smo ciliary transport, we speculated that *Ptch1* might be a candidate for macroautophagy regulation.

We and other groups previously demonstrated that the Shh ligand induces the internalization and degradation of *Ptch1* in lysosomes,

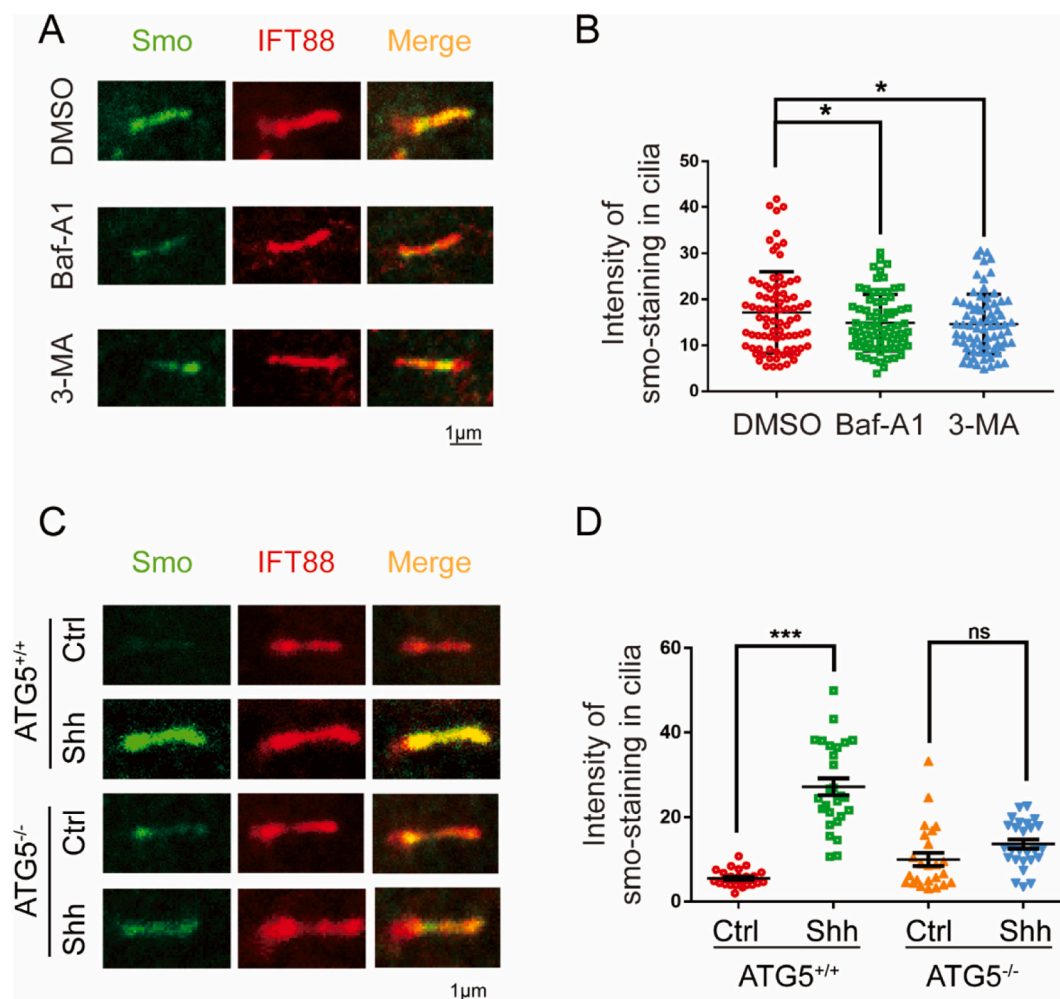
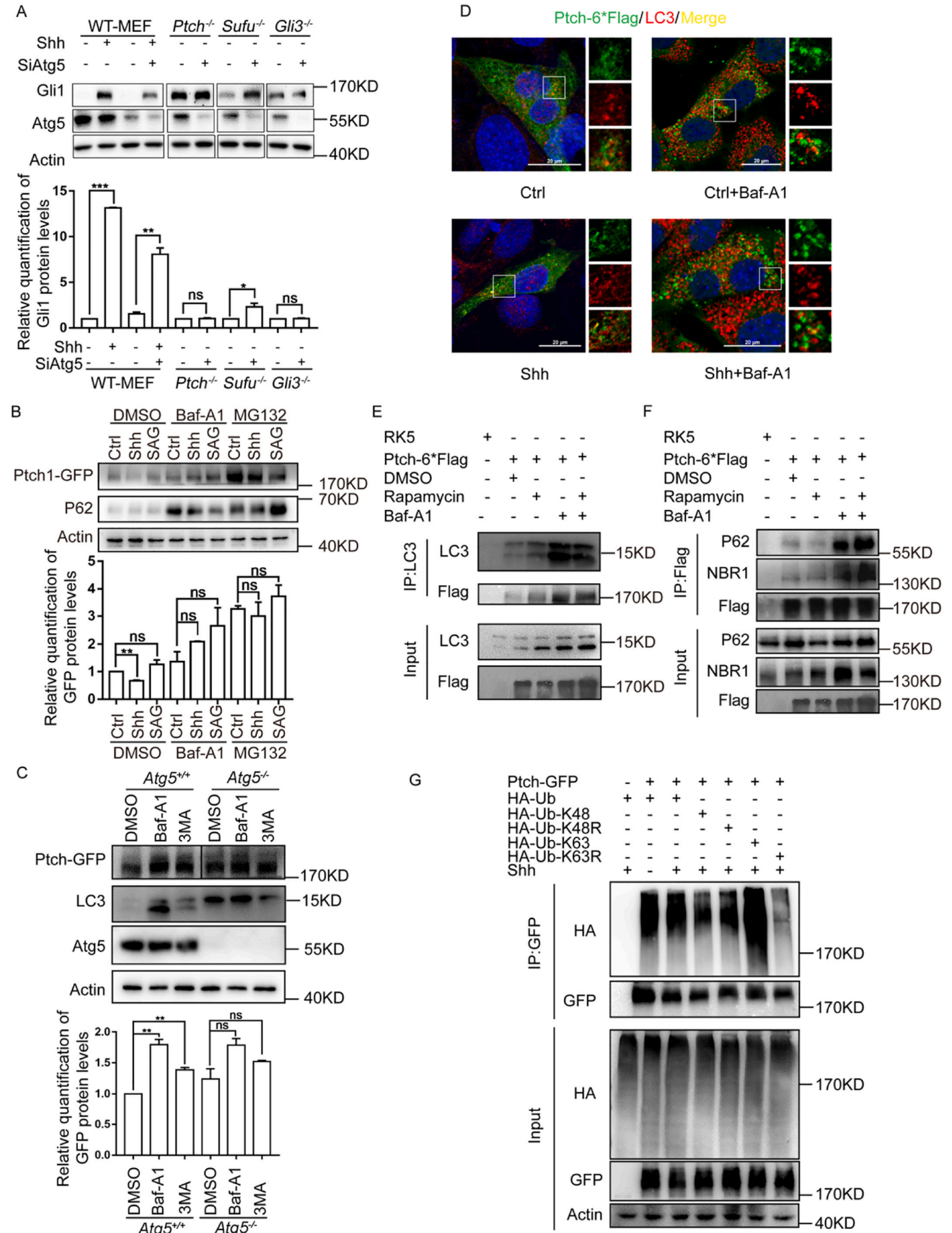


**Fig. 3.** Blocking autophagy suppressed Shh-induced transport of Smo into primary cilia. (A) Representative images of endogenous Smo immunostaining (green) in primary cilium (red, stained by anti-IFT88) in MEFs treated with BafA1 or 3-MA in presence of ShhN. (B) Quantification of anti-Smo staining in primary cilium as in (A) ( $n > 50$  in each group). (C) Immunofluorescence of Smo in *Atg5*<sup>+/+</sup> and *Atg5*<sup>-/-</sup> MEFs in the absence or presence of ShhN. (D) Quantification of anti-Smo staining fluorescence as in (C) ( $n > 25$  in each group). Data in bar graphs are expressed as mean  $\pm$  SEM. \*  $P < 0.05$ , \*\*  $P < 0.01$ , n.s. not significant.



(caption on next page)

**Fig. 4.** Macroautophagy is involved in Shh-induced Ptch1 degradation. (A) Western analysis of Gli1 expression in WT, *Ptch*<sup>-/-</sup>, *Sufu*<sup>-/-</sup> and *Gli3*<sup>-/-</sup> MEFs transfected with *Atg5* siRNAs. MEFs were treated with Shh-CM to induce Gli1 expression. Quantification of Gli1 protein level normalized on actin and represented in bar graph. (B) Western analysis and relative quantification of Ptch1-GFP protein levels under BafA1 or MG132 treatment. (C) Western analysis and relative quantification of Ptch1-GFP protein levels after blocking autophagy pathway with 3-MA or BafA1 in *Atg5*<sup>+/+</sup> and *Atg5*<sup>-/-</sup> MEFs. (D) Confocal images showing colocalization of Ptch1-6×Flag (green) with endogenous LC3-positive puncta (red) at the cytoplasm. Co-immunoprecipitation analysis of the Ptch1-LC3 (E), Ptch1-p62 and Ptch1-NBR1 (F) interaction in HEK293 cells. (G) Co-immunoprecipitation analyses of Ptch1-GFP and HA-Ub or its lysine-deficient mutants. HEK293 cells were transfected with indicated plasmids and incubated with BafA1 for 4 h before immunoprecipitation. The immunocomplexes were precipitated using anti-GFP, and blotted with anti-HA. Data in bar graphs are expressed as mean ± SEM. \* *P* < 0.05, \*\* *P* < 0.01, \*\*\* *P* < 0.001, ns not significant.

thereby allowing the downstream Shh pathway to be activated. Under serum starvation, Ptch1 protein level was decreased after Shh treatment (shown in Supplementary Fig. 1B). We speculated that macroautophagy takes part in Ptch1 degradation. When expressed in *Ptch1*<sup>-/-</sup> MEFs, Ptch1-GFP was unstable, which was degraded under Shh treatment. Pretreatment with BafA1 blocked Shh-induced reduction of Ptch1-GFP (Fig. 4B), while MG132 pretreatment accumulated Ptch1-GFP to a very high level, suggesting that autophagy and UPS both function in Ptch1 degradation. Then we blocked macroautophagy process with 3-MA and BafA1 respectively and found that Ptch1-GFP was accumulated in treated MEF cells (Fig. 4C). However, the accumulation was not obvious in treated *Atg5*<sup>-/-</sup> MEFs (Fig. 4C). To assess whether Ptch1 is engulfed in autophagosomes, we transfected Ptch1-6×Flag into MEFs and found that Ptch1-6×Flag co-localized with endogenous LC3 protein in puncta in Shh treated MEFs when the autophagy was blocked by BafA1 (Fig. 4D, the control experiment without primary antibodies was shown in supplementary Fig. 2A). Meanwhile, in HEK293 cells expressing Ptch1-6×Flag, we demonstrated that Ptch1-6×Flag interacted with LC3 and this was enhanced by BafA1 treatment (Fig. 4E). These results suggested autophagy mediated the degradation of Ptch1 receptor.

It is reported that the autophagic clearance of protein cargo requires autophagy receptors, such as p62/SQSTM1 and NBR1, which simultaneously bind both ubiquitin (Ub) in ubiquitinated cargos and autophagy-specific Ub-like proteins, LC3/GABARAP. Using co-immunoprecipitation, we observed Ptch1-6×Flag binding p62 and NBR1 under BafA1 treatment (Fig. 4F). Ptch1-6×Flag was also found to co-localize with p62 and NBR1 in cytoplasmic puncta in BafA1 treated cells (supplementary Fig. 2B and 2C). These autophagy receptors show preference to K63-linked poly-Ub chains, target K63 Ub-conjugated proteins to the autophagy/lysosomal degradation pathway [36]. Ptch1 could be ubiquitinated (supplementary Fig. 2D). To demonstrate the role of ubiquitin in the degradation of Ptch1, we forced expressed Ptch1-GFP with HA-Ub or its mutants, including Ub-K48R and Ub-K63R in which lysine 48 or 63 was replaced by arginine, and Ub-K48 and Ub-K63 in which all lysines except 48 or 63 are replaced by arginine. After BafA1 treatment, immunoprecipitation assay indicated that the ubiquitination modification of Ptch1 mainly depends on K63 of Ub (Fig. 4G), which further confirmed our hypothesis that macroautophagy participates in Shh-induced Ptch1 degradation. Moreover, less ubiquitination of Ptch1 was observed with Ub-K48R which having intact K63 residue, suggesting that Ptch1 may have complicated ubiquitin code conjugated through several different linkages.

#### 4. Discussion

Shh signaling plays a vital and diverse role in embryonic development and maintaining tissue homeostasis. Autophagy is of great significance in the elimination of large amounts of long-term proteins and organelles [37,38], but it is not clear whether autophagy selectively eliminates specific pathway molecules that regulate cell signal transduction. It is reported that macroautophagy regulates ciliogenesis through autophagic clearance of cilia-related proteins, may change Shh signal transduction [39]. Our study provides evidence that macroautophagy promotes Shh signaling through the degradation of Ptch1, a repressor receptor of Shh pathway.

In our study, Shh-induced transport of Smo into cilia and

downstream Gli1 expression was impeded when the autophagy was blocked by BafA1, 3-MA or *Atg5* knockout. The blockage is not due to the defected ciliogenesis but the obstructed degradation of Shh receptor Ptch1. Autophagy is a process of protein degradation. LC3 not only serves as a marker of autophagosomes, it is also essential for the formation of autophagosomes [40,41]. Immunofluorescence showed that Ptch1-GFP colocalized with LC3. We also found that the ubiquitination of Ptch1 mainly depends on the K63-mediated poly-Ub chain. It has been reported that the autophagy receptors, such as p62/SQSTM1 and NBR1, can bind to the K63-mediated poly-Ub chain through their Ub-associated domains (UBA) and meanwhile interact with LC3 through their LC3-Interacting Region (LIR), thereby providing a molecular link between ubiquitinated substrates and autophagosomes. Based on our results, we believe that autophagy participates in the degradation of Ptch1 and the activation of Shh pathway. Moreover, our study suggested that Ptch1 may have complicated ubiquitin code conjugated through several different linkages, which may modulate the localization or activity of Ptch1 except for its degradation.

Shh signaling play a crucial role in differentiation, proliferation and survival of cancer cells, and has been becoming a very promising target for cancer therapy. For now, vismodegib and sonidegib, which target Smo to suppress the signaling, have been approved by the FDA for the treatment of advanced basal cell carcinomas (BCC) [42]. However, those inhibitors have not demonstrated satisfactory clinical benefit in lung cancer, leukemia and pancreatic adenocarcinoma compared with the effects in BCC [43]. It has been reported that regulating autophagy facilitates the anti-tumor efficacy of vismodegib in lung adenocarcinoma, through overproduction of ROS, acceleration of apoptosis, and suppression of GLI2 [44]. This success suggested a potential approach for clinical therapy via simultaneous targeting Shh signaling and autophagy pathway.

Ptch1 is a well-known tumor suppressor, not only acts to repress Smo, but also induces apoptosis through a Smo- and Gli-independent pathway [45]. In this regard, blocking macroautophagy mediated degradation of Ptch1 is a new strategy against Shh-overexpressing tumors. Further studies will be required to elucidate the molecular mechanism of macroautophagy mediated degradation of Ptch1 and identify ideal drug targets for this strategy.

Supplementary data to this article can be found online at <https://doi.org/10.1016/j.bbamcr.2021.119124>.

#### CRedit author statement

**Xin Yang:** Investigation, Formal analysis, Writing – original draft preparation.

**Nan Jin:** Investigation, Formal analysis, Writing – original draft preparation.

**Yu Wang:** Investigation, Formal analysis, Writing – original draft preparation.

**Yixing Yao:** Methodology, Investigation.

**Yue Wang:** Investigation, Formal analysis.

**Tianyuan Li:** Investigation, Formal analysis.

**Chen Liu:** Methodology, Formal analysis.

**Tingting Yu:** Methodology, Writing – editing.

**Hao Yin:** Visualization.

**Ziyu Zhang:** Conceptualization, Validation.

**Steven Y Cheng:** Supervision, Validation.



**Shen Yue:** Supervision, Conceptualization, Writing – review and editing.

## Declaration of competing interest

The authors declare that they have no known competing financial interests or personal relationships that could have appeared to influence the work reported in this paper.

## Acknowledgments

This work was supported by grants from the Chinese National Science Foundation (81572720 to S.Y.; 81871936 to S.Y.C.; 81602431 to T.-T.Y.; 81702747 to C.L.).

## References

- [1] G. Kroemer, G. Marino, B. Levine, Autophagy and the integrated stress response, *Mol. Cell* 40 (2) (2010) 280–293.
- [2] N. Mizushima, et al., Autophagy fights disease through cellular self-digestion, *Nature* 451 (7182) (2008) 1069–1075.
- [3] Y. Yang, D.J. Klionsky, Autophagy and disease: unanswered questions, *Cell Death Differ.* 27 (3) (2020) 858–871.
- [4] Y. Chen, D. Klionsky, The regulation of autophagy - unanswered questions, *J. Cell Sci.* 124 (2011) 161–170.
- [5] T. Yorimitsu, D. Klionsky, Autophagy: molecular machinery for self-eating, *Cell Death Differ.* (2005) 1542–1552.
- [6] Y. Ichimura, et al., A ubiquitin-like system mediates protein lipidation, *Nature* 408 (6811) (2000) 488–492.
- [7] N. Fujita, et al., The Atg16L complex specifies the site of LC3 lipidation for membrane biogenesis in autophagy, *Mol. Biol. Cell* 19 (5) (2008) 2092–2100.
- [8] C. Gao, et al., Autophagy negatively regulates Wnt signalling by promoting dishevelled degradation, *Nat. Cell Biol.* 12 (8) (2010) 781–790.
- [9] G. Zaffagnini, et al., p62 filaments capture and present ubiquitinated cargos for autophagy, *EMBO J.* 37 (5) (2018).
- [10] Z. Xie, D. Klionsky, Autophagosome formation: core machinery and adaptations, *Nat. Cell Biol.* 9 (10) (2007) 1102–1109.
- [11] K.R. Parzych, D.J. Klionsky, An overview of autophagy: morphology, mechanism, and regulation, *Antioxid. Redox Signal.* 20 (3) (2014) 460–473.
- [12] N. Miao, et al., Sonic hedgehog promotes the survival of specific CNS neuron populations and protects these cells from toxic insult in vitro, *J. Neurosci.* 17 (15) (1997) 5891–5899.
- [13] M. Cobourne, Z. Hardcastle, P. Sharpe, Sonic hedgehog regulates epithelial proliferation and cell survival in the developing tooth germ, *J. Dent. Res.* 80 (11) (2001) 1974–1979.
- [14] A. Ruiz i Altaba, P. Sanchez, N. Dahmane, Gli and hedgehog in cancer: tumours, embryos and stem cells, *Nat. Rev. Cancer* 2 (5) (2002) 361–372.
- [15] R.L. Johnson, et al., Human homolog of patched, a candidate gene for the basal cell nevus syndrome, *Science* 272 (5268) (1996) 1668–1671.
- [16] D.M. Stone, et al., The tumour-suppressor gene patched encodes a candidate receptor for sonic hedgehog, *Nature* 384 (6605) (1996) 129–134.
- [17] K.C. Corbit, et al., Vertebrate smoothened functions at the primary cilium, *Nature* 437 (7061) (2005) 1018–1021.
- [18] R. Rohatgi, L. Milenkovic, M.P. Scott, Patched1 regulates hedgehog signaling at the primary cilium, *Science* 317 (5836) (2007) 372–376.
- [19] P. Ingham, A. McMahon, Hedgehog signaling in animal development: paradigms and principles, *Genes Dev.* 15 (23) (2001) 3059–3087.
- [20] M. Varjosalo, S. Li, J. Taipale, Divergence of hedgehog signal transduction mechanism between *Drosophila* and mammals, *Dev. Cell* 10 (2) (2006) 177–186.
- [21] C. Pickart, Back to the future with ubiquitin, *Cell* 116 (2) (2004) 181–190.
- [22] Y.T. Kwon, A. Ciechanover, The ubiquitin code in the ubiquitin-proteasome system and autophagy, *Trends Biochem. Sci.* 42 (11) (2017) 873–886.
- [23] S. Yue, Y. Chen, S.Y. Cheng, Hedgehog signaling promotes the degradation of tumor suppressor Sufu through the ubiquitin-proteasome pathway, *Oncogene* 28 (4) (2009) 492–499.
- [24] Yin, W.C., et al., Dual regulatory functions of SUFU and targetome of GLI2 in SHH subgroup medulloblastoma. *Dev. Cell*, 2019. 48(2): p. 167–183 e5.
- [25] A. Zhou, et al., Gli1-induced deubiquitinase USP48 aids glioblastoma tumorigenesis by stabilizing Gli1, *EMBO Rep.* 18 (8) (2017) 1318–1330.
- [26] C. Pohl, I. Dikic, Cellular quality control by the ubiquitin-proteasome system and autophagy, *Science* 366 (6467) (2019) 818–822.
- [27] Y. Chen, et al., Dual phosphorylation of suppressor of fused (Sufu) by PKA and GSK3 $\beta$  regulates its stability and localization in the primary cilium, *J. Biol. Chem.* 286 (15) (2011) 13502–13511.
- [28] Y. Zhang, et al., Regulation of Smad degradation and activity by Smurf2, an E3 ubiquitin ligase, *Proc. Natl. Acad. Sci. U. S. A.* 98 (3) (2001) 974–979.
- [29] M. Yamashita, et al., Ubiquitin ligase Smurf1 controls osteoblast activity and bone homeostasis by targeting MEK2 for degradation, *Cell* 121 (1) (2005) 101–113.
- [30] M. Yamashita, et al., TRAF6 mediates Smad-independent activation of JNK and p38 by TGF- $\beta$ , *Mol. Cell* 31 (6) (2008) 918–924.
- [31] L.Y. Tang, et al., Ablation of Smurf2 reveals an inhibition in TGF- $\beta$  signalling through multiple mono-ubiquitination of Smad3, *EMBO J.* 30 (23) (2011) 4777–4789.
- [32] M. Blank, et al., A tumor suppressor function of Smurf2 associated with controlling chromatin landscape and genome stability through RNF20, *Nat. Med.* 18 (2) (2012) 227–234.
- [33] S.C. Goetz, K.V. Anderson, The primary cilium: a signalling centre during vertebrate development, *Nat Rev Genet* 11 (5) (2010) 331–344.
- [34] Z. Tang, et al., Autophagy promotes primary ciliogenesis by removing OFD1 from centriolar satellites, *Nature* 502 (7470) (2013) 254–257.
- [35] O. Pampliega, et al., Functional interaction between autophagy and ciliogenesis, *Nature* 502 (7470) (2013) 194–200.
- [36] W.C. Shen, et al., Mutations in the ubiquitin-binding domain of OPTN/optineurin interfere with autophagy-mediated degradation of misfolded proteins by a dominant-negative mechanism, *Autophagy* 11 (4) (2015) 685–700.
- [37] N. Mizushima, Autophagy: process and function, *Genes Dev.* 21 (22) (2007) 2861–2873.
- [38] C. He, D.J. Klionsky, Regulation mechanisms and signaling pathways of autophagy, *Annu. Rev. Genet.* 43 (2009) 67–93.
- [39] I. Orhon, et al., Autophagy and regulation of cilia function and assembly, *Cell Death Differ.* 22 (3) (2015) 389–397.
- [40] T. Kirisako, et al., Formation process of autophagosome is traced with Apg8/Aut7p in yeast, *J. Cell Biol.* 147 (2) (1999) 435–446.
- [41] I. Tanida, T. Ueno, E. Kominami, LC3 conjugation system in mammalian autophagy, *Int. J. Biochem. Cell Biol.* 36 (12) (2004) 2503–2518.
- [42] G. Brancaccio, et al., Sonidegib for the treatment of advanced basal cell carcinoma, *Front. Oncol.* 10 (2020), 582866.
- [43] H. Xie, et al., Recent advances in the clinical targeting of hedgehog/GLI signaling in cancer, *Cells* 8 (5) (2019).
- [44] J. Fan, et al., Regulating autophagy facilitated therapeutic efficacy of the sonic hedgehog pathway inhibition on lung adenocarcinoma through GLI2 suppression and ROS production, *Cell Death Dis.* 10 (9) (2019) 626.
- [45] C. Thibert, et al., Inhibition of neuroepithelial patched-induced apoptosis by sonic hedgehog, *Science* 301 (5634) (2003) 843–846.